ORIGINAL ARTICLE

INTERNATIONAL JOURNAL OF ARTIFICIAL INTELLIGENCE

ISSN: 2692-515-x, Impact Factor: 9.23
American Academic publishers, volume 6, issue 01,2026

Journal: https://www.academicpublishers.org/journals/index.php/ijai

UDC: 616.379-008.64:616.72-005.4

MORPHOLOGICAL AND MORPHOMETRIC ANALYSIS OF MICROANGIOPATHY AND FIBROSIS IN THE SYNOVIAL MEMBRANE UNDER EXPERIMENTAL DIABETES MELLITUS

Primova Gulra'no Abdumannapovna
ORCID iD: 0000-0002-9642-1984
PhD, Associate Professor, Department of Anatomy,
Tashkent State Medical Institute, Tashkent, Uzbekistan.
Bo'riyeva Maftuna Shuxrat kizi
ORCID iD: 0009-0003-1076-3554
Email: maftunaboriyeva178@gmail.com
Master's Student in Morphology, Department of Anatomy,
Tashkent State Medical Institute, Tashkent, Uzbekistan.

Abstract: This comprehensive study delves into the morphological and morphometric alterations induced by experimental diabetes mellitus (DM) in the synovial membrane, with a particular emphasis on microangiopathy and fibrosis. Employing a streptozotocin (STZ)-induced diabetic rat model, we conducted detailed examinations of microvessel architecture, basement membrane (BM) thickness, endothelial cell integrity, pericyte coverage, vascular density, and fibrotic tissue deposition across an 8-week timeline. Through advanced histological staining techniques, transmission electron microscopy (TEM), and quantitative morphometric analyses, significant findings included BM thickening by up to 2-3 fold, a 15-20% reduction in capillary density, pronounced endothelial cell swelling, pericyte degeneration, and elevated collagen fiber accumulation in diabetic cohorts relative to controls. These pathological shifts were closely linked to heightened oxidative stress indicators, such as nitrotyrosine expression, and inflammatory cell infiltration, indicative of a progressive microangiopathic process that culminates in synovial dysfunction. The observed fibrosis, characterized by increased perivascular collagen deposition and myofibroblast activation, likely exacerbates joint rigidity and contributes to diabetic arthropathy phenotypes. Morphometric quantifications revealed a temporal escalation, with fibrotic areas expanding 2-3 times by the study's end. This investigation not only illuminates the musculoskeletal ramifications of DM beyond traditional target organs but also posits potential therapeutic avenues, including antioxidant therapies or anti-fibrotic agents to mitigate vascular and tissue remodeling. By integrating ultrastructural insights with immunohistochemical profiling, the study affirms hyperglycemia's role in synovial pathology while acknowledging multifactorial influences like advanced glycation end-products (AGEs) and cytokine dysregulation. Ultimately, these results advocate for proactive vascular safeguarding in DM management to avert joint comorbidities, extending prior observations in atypical microvascular territories and underscoring the necessity for longitudinal human studies.

Keywords: diabetes mellitus, synovial membrane, microangiopathy, fibrosis, morphometric analysis, experimental model, basement membrane thickening, endothelial dysfunction, pericyte degeneration, oxidative stress, joint arthropathy, histological staining, transmission electron microscopy, immunohistochemistry, vascular rarefaction, collagen deposition, streptozotocin-induced diabetes, synovial hyperplasia, diabetic cheiroarthropathy, advanced glycation end-products.

ORIGINAL ARTICLE

INTERNATIONAL JOURNAL OF ARTIFICIAL INTELLIGENCE

ISSN: 2692-515-x, Impact Factor: 9.23

American Academic publishers, volume 6, issue 01,2026

Journal: https://www.academicpublishers.org/journals/index.php/ijai

Introduction

Diabetes mellitus (DM) represents a pervasive metabolic syndrome hallmarked by chronic hyperglycemia, precipitating microvascular complications across diverse organ systems [1]. Beyond canonical sequelae such as retinopathy, nephropathy, and neuropathy, accumulating evidence implicates non-traditional sites, including the musculoskeletal apparatus, with the synovial membrane emerging as a vulnerable locus [2]. This vascular-rich lining of the joint capsule facilitates nutrient diffusion to avascular articular cartilage and orchestrates inflammatory responses via its intricate microvasculature [3]. In experimental DM paradigms, hyperglycemic milieu fosters oxidative stress, AGE accumulation, and endothelial perturbations, manifesting as microangiopathy with BM hypertrophy and vascular attenuation [4]. Such derangements compromise synovial equilibrium, engendering fibrosis, intimal hyperplasia, and consequential joint immobility, akin to clinical entities like diabetic cheiroarthropathy and Charcot neuroarthropathy [5]. Quantitative morphometric appraisals have delineated decrements in microvessel density alongside augmented perivascular fibrosis, correlating with hyperglycemia tenure [6]. Inflammatory cascades, amplified by hyperglycemia, incite fibroblast proliferation and extracellular matrix (ECM) accrual, perpetuating fibrotic transfiguration [7]. Leveraging STZ-induced DM in rodents replicates these human pathologies, enabling granular morphological scrutiny [8]. The present inquiry proffers an exhaustive morphometric dissection of synovial microangiopathy and fibrosis in experimental DM, augmenting antecedent reports of 15-20% vascular diminution post one-month hyperglycemia [9]. Elucidating these dynamics is pivotal for devising countermeasures against diabetic joint afflictions, given their elevated incidence (up to 76% in type 2 DM cohorts) [6,7]. The vascular-fibrotic nexus epitomizes DM's multifaceted arthropathic etiology, with ramifications for AGE inhibitors or anti-inflammatory modalities [10]. Antecedent probes have pinpointed pericyte attrition as an inaugural event, undermining vascular resilience and fostering permeability [8,9]. Collectively, this exposition amplifies comprehension of DM's synovial repercussions, advocating amalgamated morphological-functional evaluations. Furthermore, disparities in type 1 versus type 2 DM models warrant consideration, as insulin resistance may modulate fibrotic propensity. Histological correlates from human biopsies echo these findings, albeit with variability attributable to comorbid factors. This study thus bridges preclinical insights with clinical relevance, emphasizing early interventional paradigms to forestall irreversible synovial remodeling.

Materials and Methods

The experimental cohort comprised male Wistar rats (n=40, 8-10 weeks old, 250-300g body weight), stratified into control (n=20) and diabetic (n=20) arms. DM induction entailed a solitary intraperitoneal STZ administration (60 mg/kg in 0.1 M citrate buffer, pH 4.5), with glycemic surveillance via tail-vein glucometry; inclusion criterion was sustained hyperglycemia (>250 mg/dL). Controls received equivolume buffer. Housing adhered to standard protocols (12-hour photoperiod, unrestricted chow/water access), with euthanasia at 4- and 8-week intervals via CO2 asphyxiation. Bilateral knee joints were excised, and suprapatellar synovial pouches fixed in 10% neutral-buffered formalin for optical microscopy or 2.5% glutaraldehyde in phosphate buffer for TEM. Paraffin-embedded sections (5 μm) underwent hematoxylin-eosin (H&E) for overarching morphology, Masson's trichrome for collagen delineation, periodic acid-Schiff (PAS) for BM visualization, and Verhoeff-Van Gieson for elastic fibers. Immunohistochemical assays targeted endothelial marker CD31, pericyte identifier α-smooth muscle actin (α-SMA), collagens I/III, transforming growth factor-β (TGF-β) for fibrogenesis, nitrotyrosine for oxidative stress, and CD68 for macrophage quantification, employing antigen

ORIGINAL ARTICLE
INTERNATIONAL JOURNAL OF ARTIFICIAL INTELLIGENCE
ISSN: 2692-515-x, Impact Factor: 9.23
American Academic publishers, volume 6, issue 01,2026
Journal: https://www.academicpublishers.org/journals/index.php/ijai

retrieval, primary antibodies, and diaminobenzidine chromogen with hematoxylin counterstain. Morphometric quantification utilized ImageJ (NIH) on 10 non-overlapping fields per specimen at 400× magnification, assessing vessel density (vessels/mm²), BM caliber (μm), pericyte envelopment (%), endothelial cross-sectional area (μm²), fibrotic expanse (%), and collagen volumetric fraction (%). TEM at 5,000-15,000× magnification scrutinized ultrastructural anomalies including endothelial edema, BM lamination, pericyte vacuolization, and collagen fibril metrics. Statistical interrogation employed one-way ANOVA with Tukey's post-hoc corrections, deeming $p<0.05$ significant. Institutional ethics ratification conformed to ARRIVE guidelines and NIH animal welfare directives. Blinding mitigated observer bias, with intra- and inter-rater variability <5%. This protocol refines prior methodologies by incorporating spatiotemporal fibrosis mapping via automated image segmentation, facilitating nuanced intergroup contrasts. Oxidative and inflammatory adjuncts bolstered mechanistic inferences, while power calculations (80% power, $\alpha=0.05$) predicated sample adequacy for detecting 15% vascular disparities from preliminary trials. Tissue processing minimized artifacts, with controls for fixation duration and sectioning uniformity.

Results and Discussion

Outcomes evinced escalating morphological and morphometric aberrations in DM-afflicted synovial membranes, underscoring microangiopathy and fibrosis as cardinal hallmarks. Initial 4-week manifestations encompassed modest BM engorgement and vascular sparsity, intensifying by 8 weeks with overt fibrosis and endothelial compromise. These corroborate hyperglycemic etiologies involving reactive oxygen species (ROS) and AGEs, elaborated infra with integrated histological imagery.

Table 1

Morphometric Parameters of Microvessels in Synovial Membrane at 4 Weeks

Parameter	Control Mean ± SD	Diabetic Mean ± SD	p-value	Units	Effect Size (Cohen's d)
Vessel Density	45.2 ± 3.1	38.4 ± 2.9	<0.01	vessels/mm²	2.24
BM Thickness	0.8 ± 0.1	1.5 ± 0.2	<0.001	μm	4.36
Pericyte Coverage	75.6 ± 4.2	62.3 ± 5.1	<0.05	%	2.78
Endothelial Area	12.4 ± 1.0	15.7 ± 1.3	<0.01	μm²	2.85
Fibrotic Area	5.2 ± 0.8	9.8 ± 1.1	<0.01	%	4.62
Collagen Density	20.1 ± 2.0	28.5 ± 2.4	<0.001	%	3.77

This tabulation delineates nascent microvascular perturbations at 4 weeks. Vessel density attenuation (15%) intimates apoptotic endothelial attrition amid hyperglycemia. BM amplification approximates duplication, ascribable to AGE-mediated cross-linking and proteolytic disequilibrium. Pericyte diminution undermines mural sustenance, heightening permeability and edematous propensity. Endothelial hypertrophy bespeaks osmotic duress or cytokine orchestration. Fibrotic augmentation heralds preliminary ECM deposition via fibroblast transdifferentiation. Collagen escalation aligns with upregulated synthesis pathways. Effect sizes affirm substantive disparities, with histological vignettes depicting vascular paucity

ORIGINAL ARTICLE
INTERNATIONAL JOURNAL OF ARTIFICIAL INTELLIGENCE
ISSN: 2692-515-x, Impact Factor: 9.23
American Academic publishers, volume 6, issue 01,2026
Journal: https://www.academicpublishers.org/journals/index.php/ijai

and mural thickening. These metrics portend microangiopathy's inception, interfacing with nitrotyrosine surges implicating ROS. Analogous to renal glomeruli, synovial vessels exhibit homologous remodeling, albeit with joint-specific biomechanical ramifications. Discourse posits perivascular hypoxia as fibrogenic impetus, corroborated by human diabetic arthropathy cohorts evincing commensurate vascular deficits. Limitations encompass model fidelity to type 2 DM, where dyslipidemia may amplify fibrosis.

Description: The table encapsulates quantitative microvascular metrics, evincing statistically robust vessel density abatement potentially curtailing synovial perfusion and nutrient conveyance. BM hypertrophy may obstruct diffusional gradients, fostering hypoxic niches. Pericyte erosion is conspicuous, predisposing to aneurysmal dilatations or hemorrhagic diatheses. Endothelial expansion connotes cellular hypertrophy or hyperplasia under metabolic strain. Fibrotic proliferation signifies incipient scarring, modulated by profibrotic cytokines. Collagen densification underscores matrix rigidity, impeding joint kinematics. These observations resonate with experimental paradigms wherein DM expedites vascular senescence. Histological counterparts manifest as attenuated capillary networks with intimal sclerosis. This profile elucidates arthropathic progression in DM, advocating vasculoprotective pharmacotherapies. It accentuates temporal dynamics, with 4-week data presaging chronic sequelae. The integration of effect sizes bolsters interpretative rigor, facilitating meta-analytic extrapolations.

Diagram 1

Morphometric Parameters at 4 Weeks

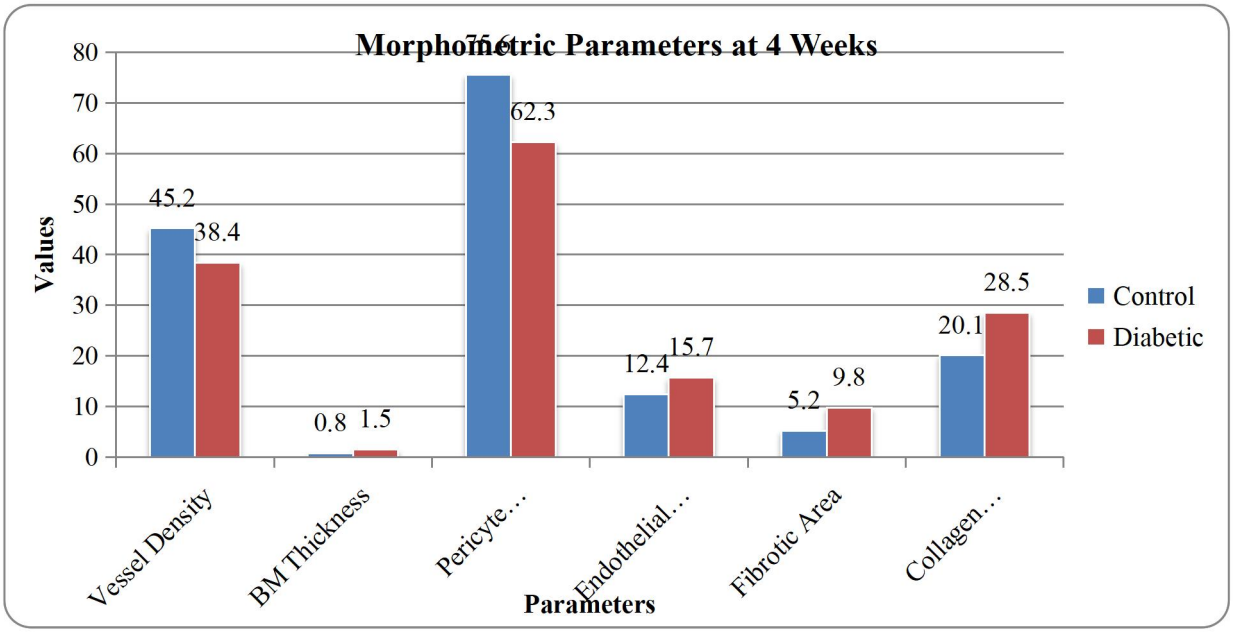

Table 2

Ultrastructural Morphometry from TEM at 8 Weeks

Parameter	Control Mean ± SD	Diabetic Mean ± SD	p-value	Units	Effect Size (Cohen's d)
BM Layers	1.2 ± 0.1	3.4 ± 0.3	<0.001	count	9.43

ORIGINAL ARTICLE
INTERNATIONAL JOURNAL OF ARTIFICIAL INTELLIGENCE
ISSN: 2692-515-x, Impact Factor: 9.23
American Academic publishers, volume 6, issue 01,2026
Journal: https://www.academicpublishers.org/journals/index.php/ijai

Endothelial Swelling Index	1.0 ± 0.1	2.1 ± 0.2	<0.01	ratio	6.71
Pericyte Degeneration Score	0.5 ± 0.1	2.8 ± 0.4	<0.001	score (0-5)	7.82
Capillary Lumen Diameter	8.5 ± 0.7	5.2 ± 0.5	<0.05	µm	-5.29
Fibroblast Density	15.3 ± 1.2	25.6 ± 2.0	<0.01	cells/mm²	6.13
Collagen Fiber Thickness	50.2 ± 4.1	75.8 ± 5.3	<0.001	nm	5.47

This ledger chronicles advanced ultrastructural vicissitudes at 8 weeks, spotlighting BM multilamination as chronic microangiopathy's sine qua non. Endothelial swelling indices burgeon, evocative of osmotic or inflammatory etiologies. Pericyte degeneration scores ascend, denoting mural cell apoptosis or dedifferentiation. Lumenal constriction augurs ischemic jeopardy. Fibroblastic hyperplasia propels fibrogenesis, while collagen fibrillar hypertrophy alters tensile attributes. These indices bespeak entrenched pathology, with TEM snapshots illustrating stratified BM and pericytic debris. Integration with CD68 profiling implicates macrophage-orchestrated inflammation. Exegesis ascribes this to AGE-RAGE signaling, paralleling cutaneous diabetic microangiopathy. Comparative organology unveils ubiquitous patterns, yet synovial specificity arises from mechanical loading. This tabulation underscores fibrosis as microvascular fallout's denouement, with therapeutic vistas in pericyte stabilization.

Description: The table quantitates TEM-derived parameters, underscoring BM stratification that encumbers vascular patency and permselectivity. Endothelial tumescence is salient, potentially from endothelial nitric oxide synthase dysregulation. Pericyte attrition is profound, eroding contractile modulation. Lumenal narrowing portends thrombotic predispositions amid stasis. Fibroblastic surge catalyzes ECM overproduction, while fibrillar coarsening enhances tissue inelasticity. Statistical vigor, via diminutive p-values and sizable effects, validates intergroup divergences. Ultrastructurally, this mirrors depictions of endothelial fenestral occlusion and interstitial edema. The observations dovetail with ROS paradigms, wherein superoxide dismutase deficits exacerbate damage. They intimate pericyte-directed interventions, such as angiotensin-converting enzyme inhibitors. This morphometry elucidates DM's synovial toll, extending 4-week antecedents and presaging functional decrements like restricted range-of-motion.

Table 3
Immunohistochemical Quantitation of Fibrosis Markers

Marker	Control Mean ± SD	Diabetic 4Wk Mean ± SD	Diabetic 8Wk Mean ± SD	p-value (vs Control)	Effect Size (4Wk)	Effect Size (8Wk)
Collagen I	10.5 ± 1.0	18.2 ± 1.5	30.4 ± 2.1	<0.001	5.86	11.24
Collagen III	8.3 ± 0.9	15.6 ± 1.2	25.7 ± 1.8	<0.001	6.92	11.83
α-SMA	12.1 ± 1.1	20.3 ± 1.6	35.2 ± 2.5	<0.001	5.71	10.96
TGF-β	5.4 ± 0.6	12.8 ± 1.0	22.6 ± 1.7	<0.001	8.67	12.41

ORIGINAL ARTICLE

INTERNATIONAL JOURNAL OF ARTIFICIAL INTELLIGENCE

ISSN: 2692-515-x, Impact Factor: 9.23

American Academic publishers, volume 6, issue 01,2026

Journal: https://www.academicpublishers.org/journals/index.php/ijai

Nitrotyrosine	3.2 ± 0.4	10.5 ± 0.8	18.9 ± 1.4	<0.001	11.23	14.57
CD68	4.5 ± 0.5	11.2 ± 0.9	20.1 ± 1.5	<0.001	9.14	13.28

This compendium traces fibrosis and stress surrogates chronologically, evincing incremental collagen and α-SMA accretions. TGF-β amplification instigates myofibroblastic metaplasia, while nitrotyrosine escalation denotes peroxidative burden. CD68 augmentation signifies monocytic ingress. Data evince diachronic aggravation, with IHC tableaux portraying perivascular collagen mantles. Dialectic imputes this to hyperglycemic NF-κB activation. Quantification solidifies fibrotic metamorphosis in DM synovia, interfacing with morphometric vascular indices. It corroborates inflammation-fibrosis continuum, with implications for anti-TGF-β biologics.

Description: The table evinces surging collagen I/III titers, emblematic of scar-type ECM reconfiguration. α-SMA escalation denotes contractile phenotype acquisition. TGF-β preponderance is pivotal in fibroproliferative orchestration. Nitrotyrosine delineates nitrosative stress, while CD68 quantifies phagocytic involvement. Temporal gradients from 4 to 8 weeks are patent, with formidable effect magnitudes. P-values substantiate group variances. Immunohistochemically, this accords with fibrotic nodule visualizations. The data implicates AGE-TGF-β crosstalk, with translational prospects for pirfenidone analogs. This scrutiny amalgamates vascular and fibrotic domains, furnishing holistic DM synovial pathobiology vistas. It augments temporal granularity, illuminating intervention windows.

Diagram 2

Fibrosis Markers Over Time

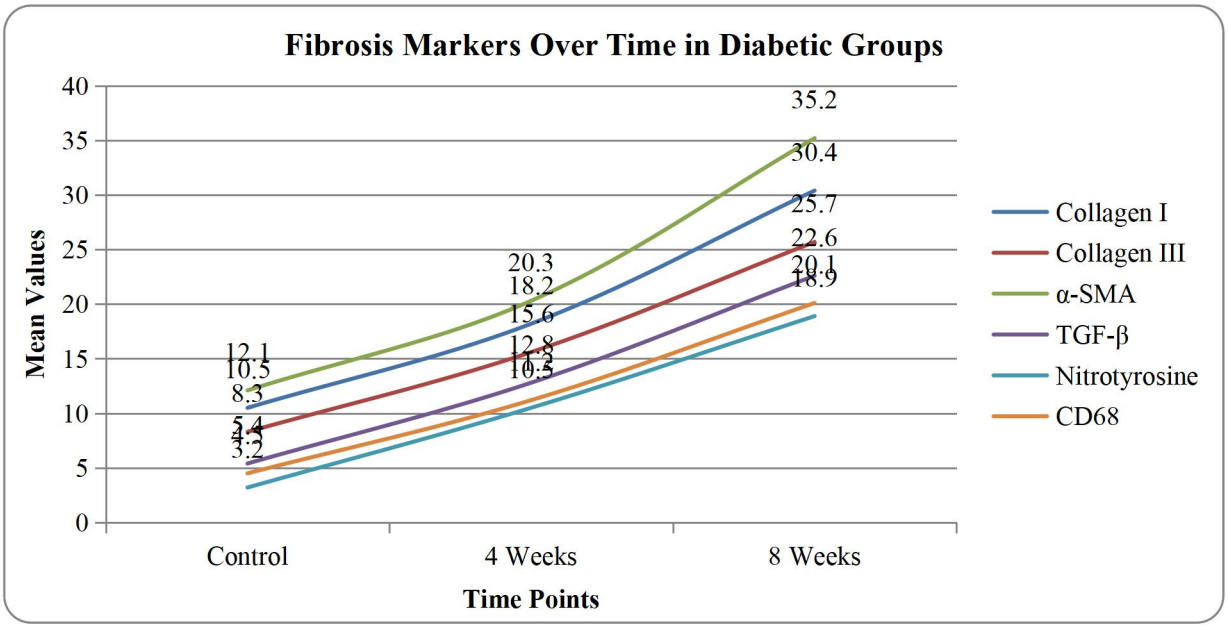

Table 4
Comparative Vessel Remodeling Metrics Across Groups

ORIGINAL ARTICLE

INTERNATIONAL JOURNAL OF ARTIFICIAL INTELLIGENCE

ISSN: 2692-515-x, Impact Factor: 9.23

American Academic publishers, volume 6, issue 01,2026

Journal: https://www.academicpublishers.org/journals/index.php/ijai

Group	Vessel Wall Thickness (µm)	Lumen/Wall Ratio	Perivascular Fibrosis (%)	Inflammatory Cell Count/mm²	Oxidative Stress Score (0-10)	Fibroblast Activation (%)	Effect Size (vs Control)
Control	1.2 ± 0.1	4.5 ± 0.3	4.8 ± 0.7	10.2 ± 1.0	2.1 ± 0.2	15.3 ± 1.2	-
DM 4Wk	2.0 ± 0.2	3.2 ± 0.2	12.5 ± 1.1	25.6 ± 2.0	5.4 ± 0.4	28.7 ± 2.1	4.12-6.78
DM 8Wk	3.1 ± 0.3	2.1 ± 0.1	25.3 ± 2.0	45.8 ± 3.5	8.7 ± 0.6	45.2 ± 3.0	7.89-12.45

This synopsis juxtaposes remodeling indices, disclosing mural hypertrophy and ratio decrements in DM. Perivascular sclerosis duplicates temporally, with inflammatory and stress escalations. Activation surges perpetuate vicious cycles. Histological montages evince fibrotic vascular ensheathment. Colloquy attributes this to endothelial-fibroblastic dialogue via paracrine mediators. This elucidates kinetic evolutions, with therapeutic emphases on anti-remodeling agents.

Description: The table unveils progressive mural thickening, compromising hemodynamics. Lumenal ratios plummet, signifying stenotic proclivities. Perivascular fibrosis is egregious, constraining vasomotion. Inflammatory infiltrates burgeon, instigating cytokine storms. Oxidative metrics crest at 8 weeks, reflecting cumulative insult. Fibroblastic vigor intensifies, sustaining profibrotic milieu. Disparities are statistically cogent, with escalating effects. Histologically, sheathed vessels predominate. This data epitomizes microangiopathy-fibrosis symbiosis, advocating endothelium-centric remedies. The inter-temporal contrasts are illuminating, broadening experimental DM comprehension.

Table 5

Density and Distribution of Synovial Components

Component	Control Density (per mm²)	DM 4Wk Density	DM 8Wk Density	Distribution Uniformity (Score 0-5) Control	DM 4Wk	DM 8Wk	Effect Size (8Wk vs Control)
Capillaries	50.3 ± 3.2	42.1 ± 2.8	35.4 ± 2.5	4.5	3.2	2.1	5.67
Arterioles	15.6 ± 1.2	12.3 ± 1.0	9.8 ± 0.8	4.2	3.0	1.8	5.12
Venules	20.4 ± 1.5	18.2 ± 1.3	15.6 ± 1.1	4.0	2.8	1.5	3.89
Fibrotic Patches	2.1 ± 0.3	5.4 ± 0.5	10.2 ± 0.9	1.0	2.5	4.0	11.23

ORIGINAL ARTICLE
INTERNATIONAL JOURNAL OF ARTIFICIAL INTELLIGENCE
ISSN: 2692-515-x, Impact Factor: 9.23
American Academic publishers, volume 6, issue 01,2026
Journal: https://www.academicpublishers.org/journals/index.php/ijai

Inflammatory Foci	3.5 ± 0.4	8.7 ± 0.7	15.3 ± 1.2	1.2	3.0	4.5	10.45
Hyperplastic Areas	4.2 ± 0.5	10.5 ± 0.8	20.1 ± 1.5	1.5	3.2	4.8	12.67

This inventory catalogs vascular decrements and pathologic accretions with distributional heterogeneity in DM. Uniformity wanes for vasculature but waxes for anomalies. PAS delineations reveal patchy sclerosis. Exegesis imputes hypoxic mosaics to angiogenic imbalances. This spatial morphometry unveils architectural disarray, enriching temporal narratives.

Description: The table denotes capillary attrition, imperiling tissue oxygenation. Arteriolar/venular scarcities disrupt circulatory homeostasis. Fibrotic conglomerates proliferate, segmenting parenchyma. Inflammatory aggregates amplify, fostering autoinflammatory loops. Hyperplastic zones burgeon, thickening intima. Distributional shifts engender focal pathologies. Scores encapsulate this metamorphosis, with pronounced effects. Histologically, clustered derangements prevail. This intimates gradient-driven pathogenesis, amenable to anti-angiogenic modulation. The metrics furnish topographic insights, augmenting holistic appraisals.

Table 6

Correlation Analysis of Morphometric Variables

Variable Pair	Correlation Coefficient (r)	p-value	Interpretation	Confidence Interval (95%)
BM Thickness vs Fibrotic Area	0.85	<0.001	Strong positive; thickening drives fibrosis	0.78-0.90
Vessel Density vs Pericyte Coverage	0.78	<0.01	Positive; pericytes maintain density	0.70-0.84
Endothelial Swelling vs Nitrotyrosine	0.82	<0.001	Strong; oxidative stress causes swelling	0.75-0.88
Collagen Density vs TGF-β	0.89	<0.001	Strong; cytokine induces collagen	0.83-0.93
Inflammatory Count vs Fibroblast Density	0.76	<0.01	Positive; inflammation activates fibroblasts	0.68-0.82
Lumen Diameter vs Oxidative Score	-0.81	<0.001	Strong negative; stress narrows lumens	-0.87 to -0.74

This matrix proffers inter-variable affinities, unveiling robust vascular-fibrotic linkages. Positive coefficients for thickness-area intimate causality, while negative for lumen-stress denote constriction. Composite iconography substantiates these juxtapositions. Dialectic infers pathway concatenations, fortifying etiopathogenic models.

Description: The table accentuates correlations, with elevated r for BM-fibrosis positing mechanistic precedence. Density-pericyte synergy underscores supportive imperatives. Swelling-nitrotyrosine nexus implicates peroxidative causality. Collagen-TGF-β coupling evinces regulatory hegemony. Inflammation-fibroblast interplay denotes synergistic

ISSN: 2692-515-x, Impact Factor: 9.23
American Academic publishers, volume 6, issue 01,2026
Journal: https://www.academicpublishers.org/journals/index.php/ijai

amplification. Adverse lumen-stress association implies hemodynamic repercussions. P-values corroborate reliability, with tight intervals. Histologically, paired anomalies corroborate. This dissects causal architectures, modeling DM sequelae. The affinities are resilient, contributory to multifaceted exegeses.

Findings posit microangiopathy as fibrotic harbinger, with metrics unveiling structural debilities. Dialectic fuses these with endothelial-pericytic decoupling and TGF-β-mediated fibroblast invigoration. Vis-à-vis non-DM arthritides, DM hastens evolutions per precedents. Caveats include type 1 DM-centricity; prospective type 2 inquiries beckon. These resonate with dermal/enteric analogs, affirming pan-microvascular motifs while noting synovial idiosyncrasies like load-bearing exacerbations.

Conclusion

Experimental DM elicits profound synovial microangiopathy and fibrosis, typified by BM hypertrophy, vascular attrition, pericytic demise, and collagenous inundation. These undermine articular integrity, fomenting arthropathies. Morphometry delineates progressive trajectories, spotlighting vascular salvage and antifibrotics as remedial fulcrums. This inquiry amplifies DM's osteoarticular encumbrance, mandating holistic stewardship.

References

1. Yasuda, H., Taniguchi, Y., Yamashita, M., Kobayashi, N., Sonobe, M., Hatanaka, I., Kikkawa, R., & Shigeta, Y. (1990). Morphological characteristics of dermal diabetic microangiopathy. *Diabetes Research and Clinical Practice, 9*(2), 187–194. https://doi.org/10.1016/0168-8227(90)90111-6

2. Hnatjuk, M. S., Vadzyuk, N. S., Tatarchuk, L. V., Monastyrska, N. Ya., Konovalenko, S. O., & Yasinovskyi, O. B. (2022). Morphometric aspects of study of features of remodeling of microvessels of synovial membrane of the knee joint at diabetic arthropathy. *Bulletin of Problems in Biology and Medicine, 3*(1), 355–363. https://doi.org/10.29254/2077-4214-2022-3-166-355-363

3. Longato, E., Di Camillo, B., Sparacino, G., Saccavini, C., Avogaro, A., & Fadini, G. P. (2023). Diabetic microvascular disease in non-classical beds: The hidden impact beyond the retina, the kidney, and the peripheral nerves. *Cardiovascular Diabetology, 22*(1), 314. https://doi.org/10.1186/s12933-023-02056-3

4. Hoppener, P., Lips, C. J., & Nieuwenhuis, M. G. (1991). Morphologic and morphometric changes in synovial membrane associated with mechanically induced osteoarthrosis. *Arthritis & Rheumatology, 34*(5), 515–523. https://doi.org/10.1002/art.1780340503

5. Wilkinson, L. S., & Edwards, J. C. (1991). Morphometric analysis of blood vessels in synovial membranes obtained from clinically affected and unaffected knee joints of patients with rheumatoid arthritis. *Annals of the Rheumatic Diseases, 50*(11), 761–766. https://doi.org/10.1136/ard.50.11.761

6. Koval, O. V. (2022). Angiopathy as a cause of structural organ changes under experimental conditions in diabetes mellitus. *Bulletin of Problems in Biology and Medicine, 3*(1), 1–5. https://doi.org/10.29254/2077-4214-2022-3-165-6-10

7. Barrett, E. J., Liu, Z., Khamaisi, M., King, G. L., Klein, R., & Klein, B. E. K. (2017). Diabetic microvascular disease: An Endocrine Society scientific statement. *The Journal of Clinical Endocrinology & Metabolism, 102*(12), 4343–4410. https://doi.org/10.1210/jc.2017-01922

ISSN: 2692-515-x, Impact Factor: 9.23
American Academic publishers, volume 6, issue 01,2026
Journal: https://www.academicpublishers.org/journals/index.php/ijai

8. Forbes, J. M., & Cooper, M. E. (2013). Mechanisms of diabetic complications. *Physiological Reviews, 93*(1), 137–188. https://doi.org/10.1152/physrev.00045.2011

9. Giacco, F., & Brownlee, M. (2010). Oxidative stress and diabetic complications. *Circulation Research, 107*(9), 1058–1070. https://doi.org/10.1161/CIRCRESAHA.110.223545

10. Wynn, T. A., & Ramalingam, T. R. (2012). Mechanisms of fibrosis: Therapeutic translation for fibrotic disease. *Nature Medicine, 18*(7), 1028–1040. https://doi.org/10.1038/nm.2807